Optimal Galaxy Shape Measurements for Weak Lensing Applications Using the Hubble Space Telescope Advanced Camera for Surveys

Yousin Park[1,2], Stefano Casertano[2] & Henry C. Ferguson[1,2]

ypark, stefano, ferguson@stsci.edu

ABSTRACT

We present three-epoch multiband (V_{606}, i_{775}, z_{850}) measurements of galaxy shapes using the "polar shapelet" or Laguerre-expansions method with the Hubble Space Telescope (HST) Advanced Camera for Surveys (ACS) data, obtained as part of the *Great Observatories Origin Deep Survey* (GOODS). We take advantage of the unique features of the GOODS/ACS Fields to test the reliability of this relatively new method of galaxy shape measurement for weak lensing analysis and to quantify the impact of the ACS Point Spread Function (PSF) on HST/ACS data. We estimate the bias introduced by the sharp PSF of the ACS on shape measurement. We show that the bias in the tangential shear due to galaxy-galaxy lensing can be safely neglected provided only well-resolved galaxies are used, while it would be comparable to the signal level (1–3%) for cosmic shear measurements. These results should of be general utility in planning and analyzing weak lensing measurements with HST/ACS data.

Subject headings: gravitational lensing—methods: data analysis–galaxies: halos—cosmology: dark matter; large-scale structure of universe

1. Introduction

The success and promise of weak lensing measurements (see Bartelmann & Schneider 2001 for a recent review) has gradually demanded new, higher-precision methods to measure galaxy shapes because the weak lensing signal is subtle. The definition of "galaxy shape" for weak lensing purposes is to some extent arbitrary, as long as it enables: (1)

[1]Department of Physics and Astronomy, The Johns Hopkins University, Baltimore, MD 21218

[2]Space Telescope Science Institute, Baltimore, MD 21218

to describe small changes in galaxy shape in sensible mathematical terms; (2) to measure galaxy shapes efficiently when implemented in practice; (3) to quantify various effects including PSF smearing; and (4) to minimize the uncertainty in the galaxy shape measurements. Recently, Bernstein & Jarvis (2002, BJ) have proposed a new method for galaxy shape measurement using Laguerre expansions. A similar approach has been independently suggested as "shapelet" methods by Refregier (2003) and Refregier & Bacon (2003), who call the Laguerre expansion "polar shapelets." A Laguerre expansion is based on the eigenfunctions of a general two-dimensional quantum harmonic oscillator, which is characterized by the oscillator's equilibrium position, its strength in two perpendicular directions and the orientation of its symmetry axis. The oscillator's strength and shape define the size, ellipticity and orientation of the Gaussian kernel. Each such set of eigenfunctions constitutes an orthonormal complete basis set that can be used to decompose a galaxy image; see BJ for more details.

The shapelet method has several advantages over other similar methods (notably the formalism by Kaiser, Squires & Broadhurst 1995) which use Gaussian-weighted second moments for shape measurement. The shapelet method: (1) applies the Gaussian weight adaptively according to the ellipticities of objects, which leads to better shape measurements for highly elliptical objects; (2) is potentially more efficient, since most operations can be performed by manipulating the shapelet coefficients of images, which can be expressed as a Hermitian matrix, instead of handling pixel data directly; and (3) allows better corrections of various effects on galaxy shape measurements, since most of those effects can be expressed as transformation matrices acting on the coefficient matrix. Since its introduction, the method has been used for cosmological weak shear measurements with ground-based observations (e.g., Jarvis et al. 2002) and morphology studies (e.g., Massey et al. 2003a). We have independently implemented the method and successfully measured the tangential shear due to galaxy-galaxy lensing as a first application (see Casertano et al. 2003).

Weak lensing measurements impose demanding requirements on observations. Ideally one would like to have deep observations over a wide area with an extremely small PSF. To control systematics, it is best if the observations are taken at multiple orientations, with galaxies appearing at different places on the detector. Multiband measurements have been adopted along with null tests to secure confidence in detection of weak lensing signals (e.g., McKay et al. 2001). The GOODS/ACS observations are perhaps the best data set yet obtained for these purposes. The general advantages of space-based observations for weak lensing are discussed by Rhodes et al. (2003) and Massey et al. (2003b). The ACS provides excellent sensitivity with a small PSF width. Observations of just a few orbits provide a high surface density of galaxies with signal-to-noise ratios (S/N) sufficient for shape measurements. Due to the supernova search strategy (Giavalisco et al. 2003), the GOODS observations were spaced into multiple epochs, separated by 40 to 50 days. Each

epoch was observed at a different orientation due to HST observing constraints. In this letter we compare galaxy shape measurements from *independent* subsets of the GOODS data in order to assess the sensitivity and robustness of the measurement technique and the quality of *HST*/ACS data for weak lensing studies.

2. Observations and Measurements

The GOODS/ACS fields are imaged in the ACS F435W, F606W, F775W, and F850LP filters (hereafter referred to as B_{435}, V_{606}, i_{775}, and z_{850}). The observations ultimately reach $S/N \sim 10$ limits $27.2, 27.5, 26.8, 26.7$ AB mag for faint galaxies; for more details of the GOODS/ACS Fields, see Giavalisco et al. (2003). The work in this letter is based on images of the first three epochs of the GOODS/ACS Chandra Deep Field South (CDF-S), which covers approximately $10' \times 16'$ at $0''.05$ pix^{-1}. Only the V_{606}, i_{775} and z_{850} band images are used in this letter. For each epoch, the total exposures are approximately 1050, 1050, and 2100 seconds, respectively. The field orientations of two successive epochs differ by 45 deg.

The **SExtractor** software (Bertin & Arnouts 1996) is used to detect and catalog objects (predominantly galaxies with some stars) and create masks for objects. The objects are extracted into individual images using the **SExtractor** segmentation map. Each object is centered in a rectangular postage-stamp image with dimensions that are at least twice the **SExtractor** extent of the object. The minimum size of the images is 32×32 pixels. We mask out surrounding objects in each of these images. For the weak-lensing measurements, we discard galaxies larger than 100×100 pixels and stars because they are almost all nearby objects that are irrelevant to lensing study. Once the postage-stamp images are prepared, we use the shapelet method to measure galaxy shapes.

The essence of the shapelet method is to approximate the intensity image of a galaxy as a finite sum of Laguerre functions with kernel properties—center, size, and shape—that match those of the image. The optimally matched kernel is the one in which the terms of the Laguerre expansion satisfy the centroid, roundness, and significance conditions, as defined in BJ. [Explicitly, these conditions mean that the (1,0), (1,1), and (2,0) terms of the Laguerre expansion vanish.] The size and shape of the galaxy are then *defined* to be the size and shape of the optimally matched kernel; BJ show that this definition obeys the correct transformation rules in the presence of translation, dilation, and shear, as may be due to weak lensing, and furthermore the definition is *optimal* in the signal-to-noise sense. In addition, the method provides a way to correct for PSF effects via a deconvolution expressed as an operation on the coefficients of the Laguerre expansion. We implemented the shapelet method within the Interactive Data Language (**IDL**). Our current implementation

successfully measures the position, size (σ), axial ratio (b/a) and position angle (PA) for $\sim 95\%$ of the galaxies brighter than $z_{850} = 24$ and $\sim 92\%$ of all galaxies down to $z_{850} = 28$; for the remaining sources, the method fails to converge. When including PSF corrections, the failure rates become $1.5 - 2$ times higher.

3. Measurement Results

The ellipticity, shear or shape of a galaxy can be represented as

$$\vec{e} \equiv (e_1, e_2) \equiv (|\vec{e}| \cos 2\phi, |\vec{e}| \sin 2\phi), \tag{1}$$

where ϕ is the position angle of the galaxy major axis and $|\vec{e}| = (a^2 - b^2)/(a^2 + b^2)$; see Miralda-Escudé (1991). Weak lensing distorts the shape slightly: $\vec{e}_{\rm dis} = \vec{\delta}_{\rm WL} \oplus \vec{e}_{\rm int}$, where $\vec{\delta}_{\rm WL}$ is the shear due to weak lensing and $\oplus$ is the shear addition operator. Here, $\vec{e}_{\rm dis}, \vec{e}_{\rm int}$ are the distorted and intrinsic shapes of the galaxy, respectively. The *shape noise*, variation in intrinsic galaxy shape, is large: $\sigma_{\rm int} = \sqrt{\langle |\vec{e}_{\rm int}|^2 \rangle} \approx 0.62$, which is substantially larger than weak lensing signal $|\vec{\delta}_{\rm WL}| \ll 1$. This makes weak lensing measurements challenging. To make matters worse, noise (predominantly due to sky background) and systematics (predominantly due to PSF) introduce *measurement errors* in shape: $\vec{e}_{\rm obs} = \vec{\delta}_{\rm PSF} \oplus \vec{\delta}_{\rm SB} \oplus \vec{e}_{\rm dis}$, where $\vec{e}_{\rm obs}$ are the shape of observed galaxy and $\vec{\delta}_{\rm PSF}, \vec{\delta}_{\rm SB}$ are measurement errors, which can be expressed as equivalent shears, due to PSF and sky background respectively. These errors demand more complicated analysis for lensing signal. For the analysis, it is essential to have good knowledge on $\vec{\delta}_{\rm SB}$ (mostly stochastic) and $\vec{\delta}_{\rm PSF}$ (mostly systematic). The multiepoch and multiband measurements provide an ideal way to assess their tendencies.

The results presented here are based on the images without PSF correction. The ACS PSF is described by Ford et al. (2003) and Pavlovsky et al. (2002); its full width at half-maximum in the GOODS images ranges from $0\farcs12$ to $0\farcs15$ depending on filter. The PSF is close to isotropic after removing the geometric distortion: the shapelet decomposition of a composite PSF yields $\sigma, b/a, {\rm PA} = (1.15 \text{ pix}, 0.985, 78\fdg1)$, $(1.17 \text{ pix}, 0.969, 59\fdg8)$, $(1.25 \text{ pix}, 0.941, 83\fdg7)$ for the $V_{606}, i_{775}, z_{850}$ bands respectively, with very small field dependence. The PSF is expected to affect the measured shapes in two ways: by broadening the galaxy image, making the galaxy look larger and rounder; and by imparting a preferential angle to the apparent orientation, a consequence of the slight anisotropy of the PSF itself. The former affects primarily the estimate of the susceptivity of galaxy images to gravitational distortion and will not introduce a spurious lensing signal or change it to first order. On the other hand, a possible bias on the observed orientation could add directly onto the measured signal, and therefore can be potentially problematic. In order to estimate the

possible bias introduced by the PSF, we compare $\langle\vec{e}\rangle$, the average galaxy shape over a large number of galaxies in different bands and in different epochs. Any systematic PSF dependence would manifest itself as a difference in the average values of the ellipticity components. Measurements in different epochs are especially significant, since the PSF rotates between epochs.

For the band-to-band comparison in shape measurement, we use a combined three-epoch mosaic for each band; the image catalog is obtained from the z_{850} band image and contains ~ 25000 objects. The galaxy masks obtained from the z_{850} band image are used for the other bands as well. We limit our comparison to galaxies with $22 < z_{850} < 26$ for which the shapelet measurement succeeds in all three bands. We divide the galaxies into bright ($22 < z_{850} < 24$) and faint ($24 < z_{850} < 26$), and into large ($\sigma_V > 2.5$ pix) and small ($\sigma_V < 2.5$ pix), where σ_V is the Gaussian size of the galaxy in the V_{606} band. Figure 1 presents a qualitative comparison of axis ratios measured in the V_{606} and i_{775} bands. The axis ratios are generally in good agreement for all magnitude and size cuts. Small galaxies appear to be rounder than larger ones regardless of brightness, presumably as a consequence of PSF dilution. A closer look indicates that galaxies look slightly rounder in the i_{775} band than in the V_{606} band, in agreement with the slightly larger PSF in the former band. Similarly, the position angle (not shown) compares well on average between the bands, with no net difference and a dispersion that increases for fainter, smaller, and rounder galaxies, as might be expected since the position angle is more difficult to measure for such galaxies. These qualitative comparisons show that the shapelet method works generally well on real galaxy images.

However, more important for weak lensing studies is a *quantitative* comparison of the ellipticity components measured on galaxies as a function of band and epoch. The ellipticity components e_1, e_2 (defined in Eq. 1) are the quantities used in weak lensing; systematic differences, as could be due, e.g., to PSF or to pixellation effects, would affect directly the ability to carry out weak lensing measurements. Figure 2 shows the band-to-band comparison of the ellipticity components for the large ($\sigma_V > 2.5$), faint ($24 < z_{850} < 26$) galaxies in Figure 1. We average the difference in ellipticity components for the galaxies in Figure 2 , and find $\langle\vec{e}(i_{775})\rangle - \langle\vec{e}(V_{606})\rangle = (0.0003 \pm 0.0036, 0.0054 \pm 0.0035)$, $\langle\vec{e}(z_{850})\rangle - \langle\vec{e}(V_{606})\rangle = (-0.0004 \pm 0.0039, -0.0144 \pm 0.0039)$. Thus, the net difference between ellipticities measured in the V_{606} and i_{775} bands is $\sim 0.5\%$; between the V_{606} and z_{850} bands is $\sim 1.4\%$. These net differences are almost entirely due to the PSF, and are more significant in the z_{850} band because of the larger, less round PSF.

The most direct test of the stability of shape measurements can be obtained by comparing measurements in the same band but at different epochs. We can only carry out such

a test for the z_{850} band images, since in the other bands not enough images were taken at each epoch for a good rejection of cosmic rays. At different epochs, the GOODS/ACS fields put galaxies on different pixel positions, and the detector rotates by 45 deg between consecutive epochs. The images have slightly different sky backgrounds, and the **SExtractor** segmentation maps for the galaxies differ from epoch to epoch due to the effects of noise. PSF anisotropies and variations over time will distort galaxy shapes differently in different epochs, as will the geometric distortion of the camera and the appearance of hot pixels, unrejected cosmic rays, and so on. As each single-epoch image is shallower than the combined image, the catalog for the single-epoch images is about half the size of the three-epoch catalog. The comparison of ellipticity components between epochs is shown in Figure 3, limited to galaxies with size $\sigma_z > 3$ pix. There is good agreement between the ellipticity components measured in different epochs. The scatter between each pair of epochs is comparable, suggesting that the variation in each object's measurement is primarily due to sky background. Since the PSF is not perfectly round, it introduces bias. For the galaxies in Figure 3, we obtain $\langle\vec{e}(\mathrm{Epoch2})\rangle - \langle\vec{e}(\mathrm{Epoch1})\rangle = (-0.0175 \pm 0.0073, 0.0158 \pm 0.0074)$ and $\langle\vec{e}(\mathrm{Epoch3})\rangle - \langle\vec{e}(\mathrm{Epoch2})\rangle = (-0.0153 \pm 0.0070, 0.0116 \pm 0.0070)$, which indicates a systematic change of $\sim 2\%$ in $\langle\vec{e}\rangle$ between epochs. This change is consistent with the change in the PSF on the sky—due to the rotation of the field of view between epochs—and implies that, even for ACS data, correction for PSF effects is necessary for cosmic shear measurements (especially with the z_{850} band images), where the signal is typically 1–3%.

The situation is different for galaxy-galaxy lensing shear measurements, which are expressed in terms of the tangential ellipticity $e_+ \equiv |\vec{e}| \cos 2\theta$, where θ is the angle between the major axis of a source and the line connecting its center to the center of a lensing galaxy. We find no statistically significant correlation between ellipticity change and position in the detector, implying that the effect of the PSF is constant over the field of view. Therefore the PSF-induced difference in ellipticity can be expected to average out, due to the random placement of lens-source pairs. Indeed, we find that the epoch-to-epoch difference in $\langle e_+\rangle$ for the lens-source population used by Casertano et al. (2003) is less than 0.01%, consistent with the noise level and much smaller than the signal they detect, which drops to $\sim 0.2\%$ at large separations. We find similarly that the difference in $\langle e_+\rangle$ between bands is less than 0.01%.

In order to quantify the effect of PSF on shear measurements, we convolve the galaxy images with the composite ACS PSF in the V_{606} band, repeat the shape measurements and compare the results with the original. The effect of the PSF on the shape of a well-resolved galaxy ($\sigma_{\mathrm{galaxy}} \gtrsim 2\sigma_{\mathrm{PSF}}$) is expected to be small, scaling roughly as $(\sigma_{\mathrm{PSF}}/\sigma_{\mathrm{galaxy}})^2$. A round PSF will make a regular galaxy larger and rounder, but will not change its orientation. Indeed, we find that PSF convolution makes galaxies larger and slightly rounder, with a

change that decreases with increasing galaxy size. Due to the anisotropy of the PSF, the convolution does induce some error in e_1, e_2, but the scatter is substantially smaller than seen in the band-to-band or epoch-to-epoch comparisons. For the galaxies with $24 < z_{850} < 26.5$ and $\sigma_V > 2.5$, we find the difference in $\langle \vec{e} \rangle$ is $\delta\vec{e} = (-0.0044 \pm 0.0020, -0.0004 \pm 0.0020)$. This bias is associated with the slight anisotropy of the PSF; if uncorrected, it would induce an ellipticity correlation at the level of $\sim \delta\vec{e}/2 \approx 0.2\%$, small but not negligible in some cases of cosmological weak shear measurement. As for the tangential shear measurements, the bias is less than 0.01% by the tangential averaging, and therefore can be safely neglected. Therefore in ACS data, the PSF correction (at least for the V_{606} band) is not essential for the shear measurement of galaxy-galaxy lensing provided only well-resolved galaxies are used.

Finally, we have carried out a blind test to determine whether we could recover a known shear. We distort a part of the z_{850} band image with 2% shear in various directions, and compare the shapes of galaxies in the sheared images with original shapes. We can recover each component of the induced 2% shears with relative errors of $\lesssim 10\%$ by comparing ~ 3000 galaxies in the images used in the test.

4. Discussion

We have presented shape measurements of galaxies in HST/ACS data using the Laguerre-expansion method. Though more tests of the PSF deconvolution step remain, the results here indicate that the impact of the PSF on galaxy shape measurements with these data are not the limiting factor for tangential shear measurement due to the superb resolution of HST/ACS, provided the galaxies are well resolved. The level of PSF-induced bias appear to be acceptable for tangential shear measurements, provided the background source galaxies are limited to $z_{850} < 26.5$ and $\sigma_V > 2.5$ pix in our case. Our method and result can be applied to different ACS data sets for quick tangential shear measurement.

Though the method proposed by BJ is simple and elegant, we have found that it needs some modification and adjustment in practice. We have done extensive tests with simulated galaxy images to assess the impacts of such effects as different pixel scales and choices of drizzling parameters. Improvement of current implementation is also underway to reduce the failure rate. The detailed implementation procedures and test results will be presented in a future article. In addition to the measurement of tangential shear due to galaxy-galaxy lensing, we intend to apply this technique to cosmological weak shear measurement, where the impact of PSF effect is expected to be larger. The depth of the GOODS/ACS Fields is ideal for such measurement, although the relatively small field of view (by ground-based standards) limits the applicability to relatively small spatial scales. The deepest V_{606} band

images provide ~ 20 background sources per square arcmin with $z > 2$ and $S/N > 15$, which we anticipate will be be sufficient for measuring the trend of the weak shear amplitude on arcmin scales with redshift. Beyond measuring galaxy shapes for weak lensing, the the shapelet method is a potentially valuable tool for studying the morphological evolution of galaxies.

We are grateful to GOODS Team, especially Tomas Dahlen and Swara Ravindranath for their assistance in generating special catalogs for the tests described in this letter. We thank Norman Grogin for his help with the blind test for image distortion. Support for this work was provided by NASA through grant GO09583.01-96A from the Space Telescope Science Institute, which is operated by the Association of Universities for Research in Astronomy, under NASA contract NAS5-26555.

REFERENCES

Bartelmann M. & Schneider, P. 2001, Phys. Rep., 340, 291

Refregier, A. 2003, MNRAS, 338, 35

Refregier, A. & Bacon, D. 2003, 338, 48

Bernstein, G. M. & Jarvis, M. 2002, AJ, 123, 583 (BJ)

Bertin, E. & Arnouts, S. 1996, A&AS, 117, 393

Casertano, S., Park, Y., Ferguson, H. C., Somerville, R. S., Moustakas, L. & Fassnacht, C. D. 2003, ApJ submitted

Ford, H. C., et al. 2003, Proc. SPIE, 4854, 81

Giavalisco, M. et al. 2003, ApJ submitted

Jarvis, M., Bernstein, G. M., Fischer, P., Smith, D., Jain, B., Tyson, J. A. & Wittman, D. 2002, preprint (astro-ph/0210604)

Kaiser, N., Squires, G. & Broadhurst, T. 1995, ApJ, 449, 460

Massey, R. J., Refregier, A. R., Conselice, C. J. & Bacon, D. J. 2003a, preprint (astro-ph/03014491)

Massey, R. J., Rhodes, J., Refregier, A., Albert, J., Bacon, D., Bernstein, G., Ellis, R., Jain, B., McKay, T., Perlmutter, S. & Taylor, A. 2003b, preprint (astro-ph/0304418)

McKay, T. A., et al. 2001, preprint (astro-ph/0108013)

Miralda-Escudé, J. 1991, ApJ, 380, 1

Pavlovsky, C., et al. 2002, ACS Instrument Handbook Version 3.0, (Baltimore: STScI).

Rhodes, J., et al. 2003, preprint (astro-ph/0304417)

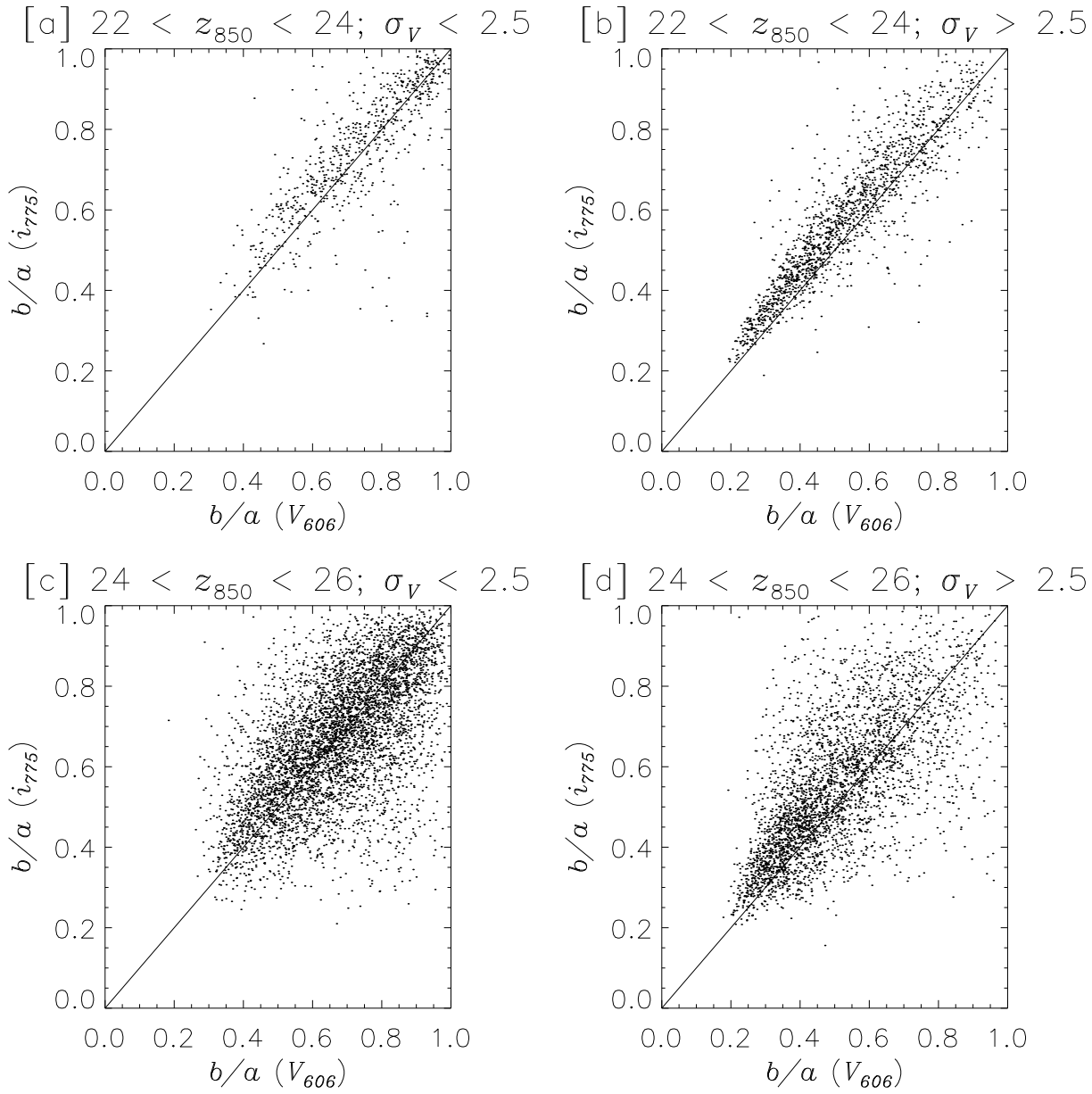

Fig. 1.— Comparison of axis ratios between the V_{606} and i_{775} bands for different magnitude and size cuts. The σ_V and z_{850} are the size of a galaxy in the V_{606} band and its magnitude in the z_{850} band respectively.

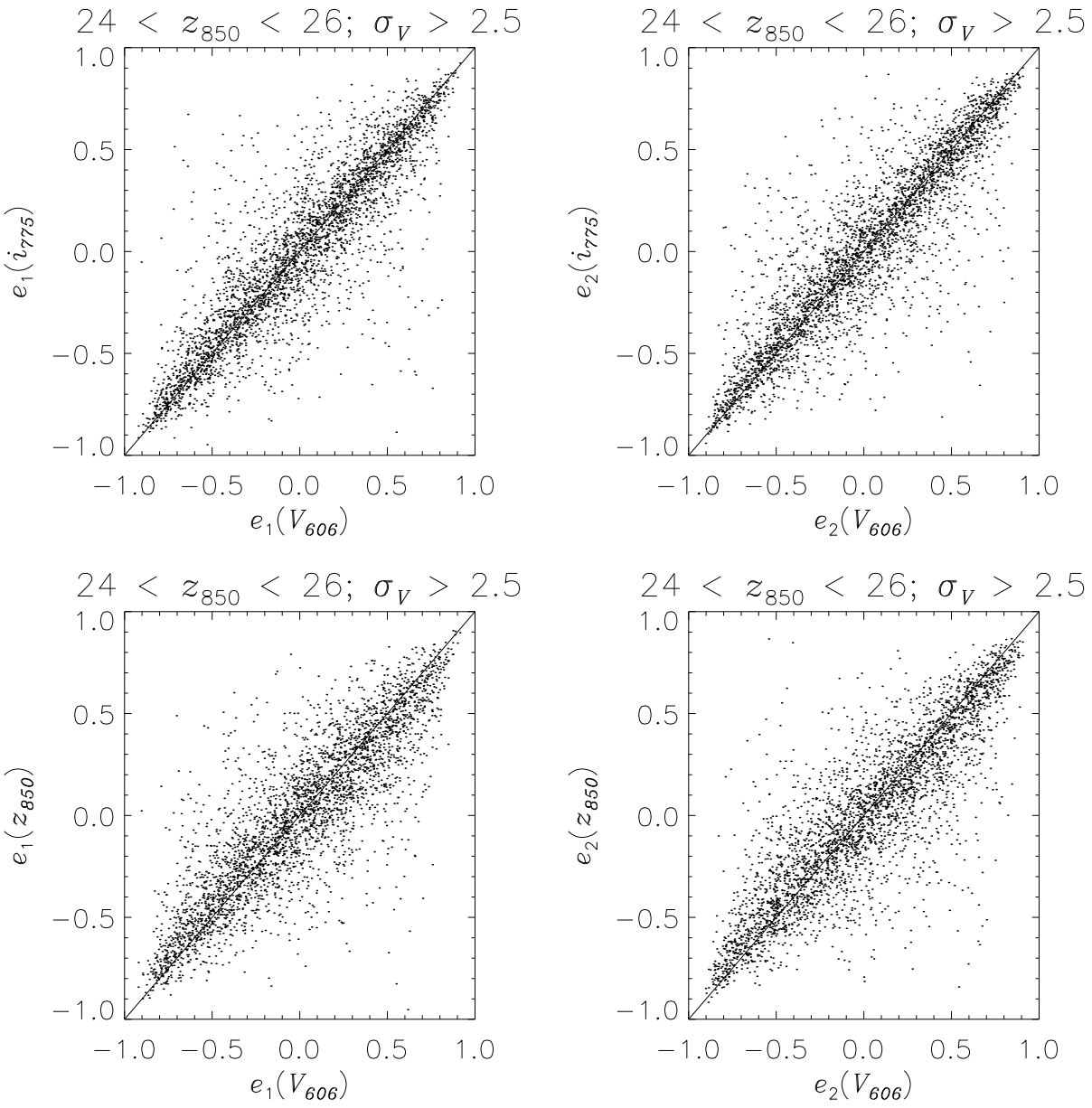

Fig. 2.— Comparison of ellipticity components in the V_{606}, i_{775}, z_{850} bands for large ($\sigma_V > 2.5$ pix) and faint ($24 < z_{850} < 26$) galaxies. The σ_V and z_{850} are the size of a galaxy in the V_{606} band and its magnitude in the z_{850} band, respectively.

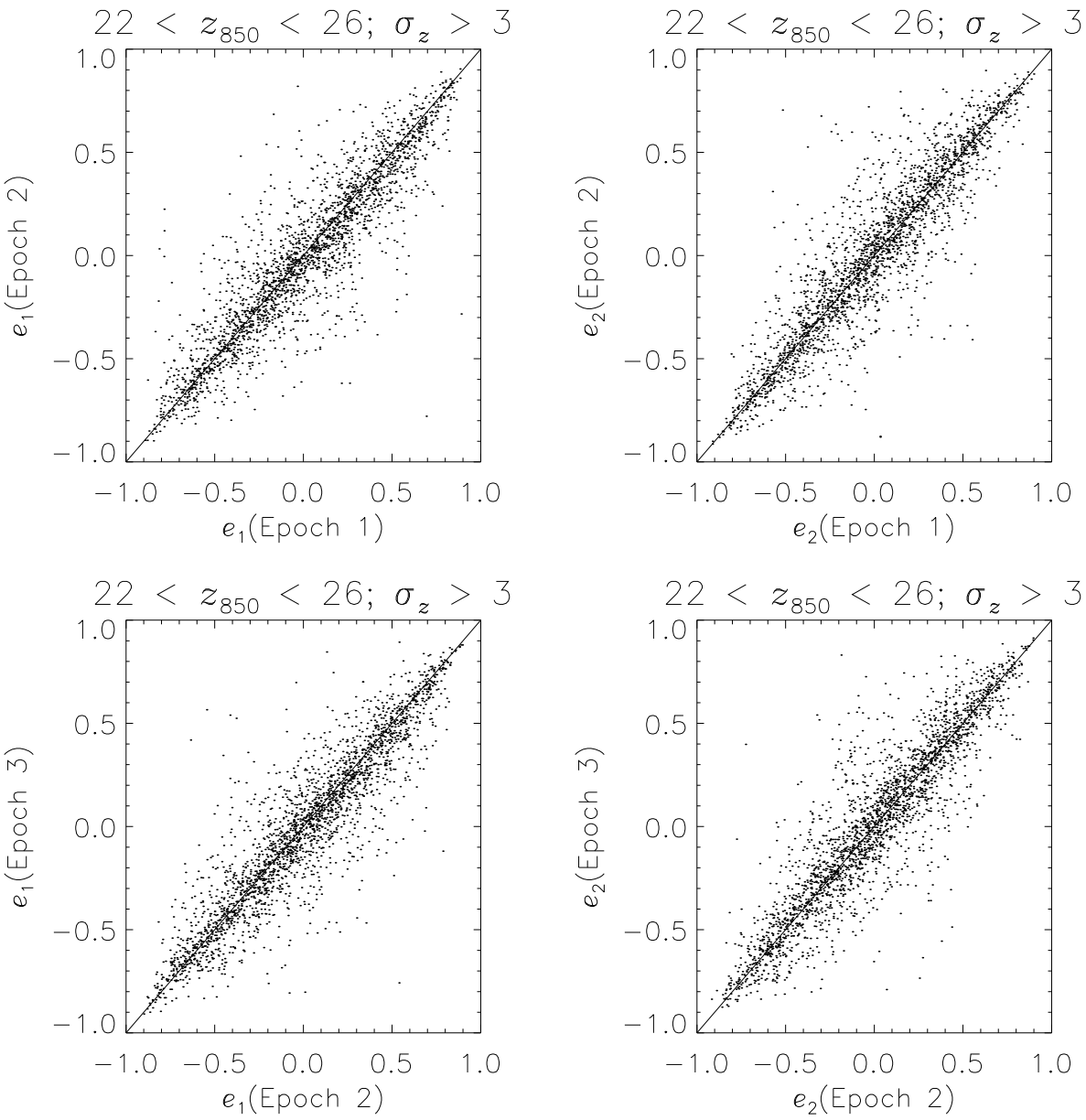

Fig. 3.— Comparison of ellipticity components among the first three epochs in the z_{850} band for large ($\sigma_z > 3$ pix) galaxies. The σ_z and z_{850} are the size of a galaxy and its magnitude in the z_{850} band.